External Joint Torques Estimation for a Position-Controlled Manipulator Employing an Extended Kalman Filter

Loris Roveda[1], Daniele Riva[2], Giuseppe Bucca[2], Dario Piga[1]

***Abstract*— Industrial robots are required to interact with the surrounding environment to perform a given task (*e.g.*, an assembly task). However, standard industrial robots are commonly position-controlled. Therefore, there is the need to implement an outer compliance controller to guarantee a safe interaction. Such compliance controllers require force/torque measurements to close the loop, and most of the industrial manipulators available on the market do not have embedded force/torque sensor(s), requiring additional efforts (*i.e.*, additional costs and implementation resources) for such integration in the robotic setup. To provide a standard industrial sensorless position-controlled robot with the capabilities to execute an interaction task, the proposed paper defines an external joint torques observer for the implementation of an outer sensorless compliance controller. More in detail, exploiting the resulting position-controlled robot dynamics, an Extended Kalman Filter (EKF) is proposed to estimate the external joint torques. Exploiting such an estimation, an outer impedance controller can be designed, providing a position/velocity reference to the inner position controller. The described approach has been validated with experiments on a Franka EMIKA panda robot. A human operator interacts with the controlled robot, applying external wrenches (*i.e.*, both Cartesian forces and torques). The resulting external joint torques are estimated making use of the proposed EKF, comparing the achieved results with the signals provided by the joint torque sensors of the Franka EMIKA panda robot (measurements used as a baseline for validation purposes). Experimental results show the capabilities of the proposed control framework in estimating the applied external joint torques while implementing a position control-based compliance controller.**

I. Introduction

A. Context

Within the Industry 4.0 paradigm, robots have to provide a flexible solution, adapting to (partially) new tasks and production, while guaranteeing the quality of the application [1]. Considering interaction tasks, there is the need to implement a compliant behavior for the controlled robot to achieve a safe interaction [2]. Common compliant controllers, however, make use of expensive sensors to be integrated in the robotic cell [3]–[5], *i.e.*, increasing the hardware costs and the setup time. Therefore, interaction forces/torques observers have been investigated to solve this issue. In the following, the state of the art related to this topic is analyzed.

The work has been developed within the project ASSASSINN, funded from H2020 CleanSky 2 under grant agreement n. 886977.

[1] Loris Roveda, and Dario Piga are with Istituto Dalle Molle di studi sull'Intelligenza Artificiale (IDSIA), USI-SUPSI, Lugano, Switzerland loris.roveda@idsia.ch

[2] Daniele Riva, and Giuseppe Bucca are with Politecnico di Milano, Department of Mechanical Engineering, Milano, Italy

B. Related work

The research community pays much attention to the achievement of a stable interaction between sensorless robots and the environment, employing efforts in developing sensorless methodologies to estimate the interaction between the robot and its environment. This research area is strongly connected with the main aim of this paper, since the proper estimation of the established interaction between the robot and its environment is required to design a stable and high-performance interaction controller for a sensorless robot. Some approaches [6] focus on the the derivation of high-accuracy models which are then used to estimate the interaction wrench during the task execution. On top of such methodologies, *disturbance observers*-based solutions are developed, estimating the external wrench applied to the manipulator exploiting the available modeling. In [7], a nonlinear disturbance observer is proposed to estimate the external interaction, allowing the possibility to consider the intrinsic non-linearities of the robotic systems. This method guarantees the stability of the disturbance observer by properly tuning its design gains taking into account the physical parameters and constraints (*e.g.*, maximum joint velocities) of the robot. A more general approach is developed in [8], where a disturbance state observer is coupled with machine learning techniques, employed to identify a task-oriented dynamic model. The use of a learning-based approach prevents an analytical modeling of the robot dynamics (such as joints friction or Coriolis effects). To deal with modeling errors, a parametric dynamics robot model coupled with machine learning techniques is proposed in [9]. A two-layer modeling is implemented with the combination of rigid-body dynamics (RBD) and a compensator trained with multilayer perception (MLP), improving the model accuracy w.r.t. each of the two considered modeling methodologies taken individually. To perform the interaction force estimation, such a modeled dynamics is then exploited in a disturbance Kalman filter based on a time-invariant composite robot model, providing robust estimation w.r.t. modeling uncertainty. In order to avoid the use of acceleration measurements and the computation of the inverse of the robot inertia matrix (resulting in amplification of the measurements noise), in [10] a sensorless admittance control scheme is proposed exploiting a generalized momentum-based disturbance observer to model a linear environment dynamics. A radial basis neural networks approach (RBNN) is used to compensate the model uncertainties. Other state of the art methods structure the identification as an *optimization problem*. A different

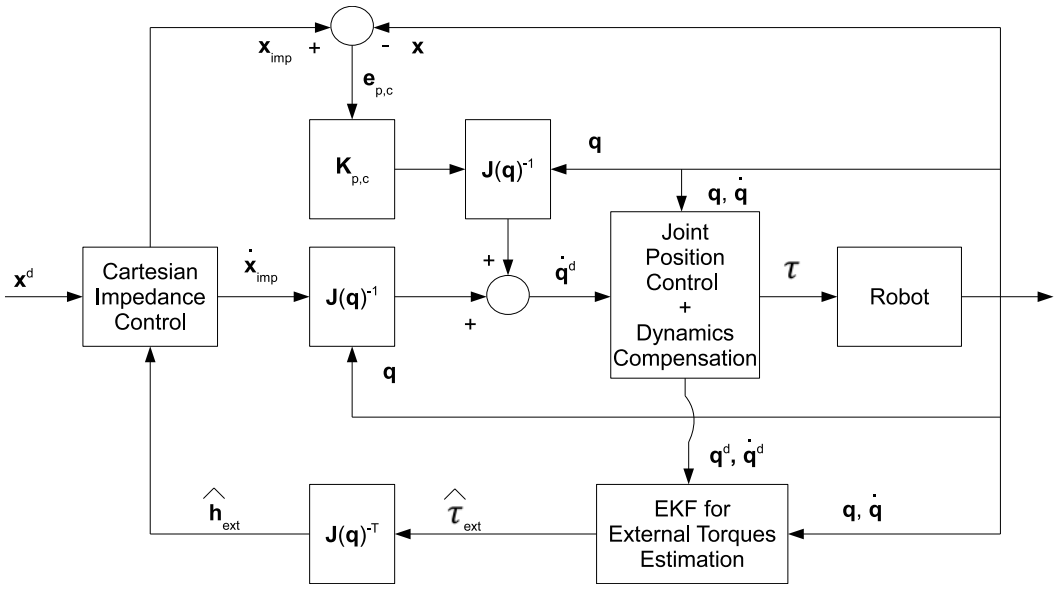

Fig. 1: Proposed control schema. The outer impedance controller and the inner position controller with robot dynamics compensation are highlighted. The proposed EKF providing the estimate of the external joint torques $\widehat{\boldsymbol{\tau}}_{ext}$ is given.

methodology that shows a deep connection with the generalized momentum-based approach is developed in [11]. The filtered dynamic equations are combined with a recursive least-square estimation algorithm to provide a smooth external force estimation. Friction models, such as Coulomb friction, show uncertainties related to the joint velocity, especially when such velocities are close to zero (*i.e.*, within the friction cone). Another contribution proposed to solve in real-time a convex optimization problem, estimating the reaction force taking into account the aforementioned Coulomb friction uncertainties [12]. Different types of *virtual sensors* based on high-performance dynamic model calibration have been also proposed. A task-oriented calibrated robot dynamic model, which includes also the thermal state of the robot manipulator, is designed in [13]. The proposed dynamic model is calibrated by means of a two-stage optimization algorithm, which provides suitable paths later combined in exciting trajectories. The estimation of the external force is obtained, using the residual method, as difference between the modeled and measured torques. *Artificial Intelligence* has been also investigated to *map the interaction* between the robot and the environment. Considering the scenario of working with soft tissue, in [14] the interaction is modeled as a visco-elastic system. The design of the external force observer is based on a Lyapunov time-varying equation. Considering a bilateral tele-operation system, in order to estimate the interaction forces between the slave manipulator and the environment, an online sparse Gaussian process regression (OSGPR) approach is proposed in [15]. The developed approach does not need any previous knowledge of the slave manipulator dynamic model, avoiding the use of the inverse of Jacobian transpose. The generalized robot model is obtained through offline training exploiting previously acquired datasets. Other external sensors can be used instead of force sensors to acquire useful data to estimate the interaction force. In [16], exteroceptive sensing (*i.e.*, a depth camera) is used for the detection of contacts, while the residual method is deployed to evaluate the external joint torques. This approach provides a reliable estimation of the exchanged force at the contact point even in the scenario of multiple contact ports. Optical Coherence Tomography (OCT) images have been also exploited for the estimation of the interaction. OCT images have been classified with a Neural Network in [17]. The network is trained on images from a Finite Element Method (FEM) simulation of the deformed sclera, while a Bayesian filter is used to parameterize the model. In [18], instead, Convolutional Neural Networks and Long-Short Term Memory networks are used to process the spatio-temporal information included in video sequences to provide an estimation of the interaction force.

C. Paper contribution

Considering the above described context (*i.e.*, sensorless position-controlled industrial manipulators performing interaction tasks), this paper proposes an external joint torques observer. For such a purpose, an Extended Kalman Filter (EKF) is defined, without requiring the use of any additional external sensor. The proposed EKF relies on the resulting position-controlled robot dynamics. The provided estimation is then used to close an outer compliance control loop. To validate the proposed approach, the derived EKF and the considered control schema have been implemented on a Franka EMIKA panda robot. The internal robot joint torque sensors have been employed to acquire the external joint torques to be used as a baseline for comparison with the estimated external joint torques (provided by the designed EKF). Experimental results show the accuracy of the performed estimation resulting in limited errors, demonstrating the feasibility of the proposed control architecture in real sensorless robotic applications.

II. METHODOLOGY

In order to provide to a sensorless position-controlled industrial robot the capabilities to interact with the surrounding environment, the control framework in Figure 1 is proposed. The inner position control is highlighted. Such a controller takes as an input the joint reference signals, generated (exploiting the inverse kinematics relation at the velocity level) by the outer Cartesian compliance controller. To implement the target compliant behavior, the outer controller takes as an input the estimation of the interaction wrench. In this paper, such an estimation is obtained by means of the external joint torques provided by the proposed EKF. In the following, the employed control schema and the EKF are described.

III. ROBOT CONTROLLER

A. Outer impedance control

As described in [19], an impedance controller can be designed to perform a compliant task, providing with a reference the inner position controller. On the basis of the interaction force acting on the manipulator, impedance control allows to calculate the robot accelerations $\ddot{\mathbf{x}}_{imp} = [\ddot{\mathbf{p}}; \ddot{\boldsymbol{\varphi}}_{cd}]$ (where $\ddot{\mathbf{p}}$ are related to the traslational degrees of freedom - DoFs -, and $\ddot{\boldsymbol{\varphi}}_{cd}$ are related to the rotational DoFs described by the intrinsic Euler angles representation):

$$\begin{aligned} \ddot{\mathbf{p}} &= \mathbf{M}_t^{-1} \left(-\mathbf{D}_t \dot{\mathbf{p}} - \mathbf{K}_t \Delta\mathbf{p} - \mathbf{f}_t\right) \\ \ddot{\boldsymbol{\varphi}}_{cd} &= \mathbf{M}_\varphi^{-1} \left(-\mathbf{D}_\varphi \dot{\boldsymbol{\varphi}}_{cd} - \mathbf{K}_\varphi \boldsymbol{\varphi}_{cd} + \mathbf{S}_\omega^T(\boldsymbol{\varphi}_{cd})\boldsymbol{\tau}_\varphi\right) \end{aligned} \tag{1}$$

Considering the traslational part of the impedance control, $\mathbf{M}_t$ is the target mass matrix, $\mathbf{D}_t$ is the target damping matrix, $\mathbf{K}_t$ is the target stiffness matrix, $\mathbf{f}_t$ is the external forces vector. $\mathbf{p}$ is the actual Cartesian positions vector, while $\Delta\mathbf{p} = \mathbf{p} - \mathbf{p}^d$, where $\mathbf{p}^d$ is the target positions vector. Considering the rotational part of the impedance control, $\mathbf{M}_\varphi$ is the target inertia matrix, $\mathbf{D}_\varphi$ is the target damping matrix, $\mathbf{K}_\varphi$ is the target stiffness matrix. $\boldsymbol{\varphi}_{cd}$ is the set of Euler angles extracted from $\mathbf{R}_c^d = \mathbf{R}_d^T\mathbf{R}_c$, describing the mutual orientation between the compliant frame $\mathbf{R}_c$ (coincident with the robot end-effector reference frame) and the target frame $\mathbf{R}_d$. $\boldsymbol{\tau}_\varphi$ is the external torques vector referred to the target frame. Matrix $\mathbf{S}_\omega(\boldsymbol{\varphi}_{cd})$ defines the transformation from Euler angles derivatives to angular velocities $\boldsymbol{\omega} = \mathbf{S}_\omega(\boldsymbol{\varphi}_{cd})\dot{\boldsymbol{\varphi}}_{cd}$ [20]. The six DoFs impedance control results, therefore, in:

$$\mathbf{M}\ddot{\mathbf{x}}_{imp} + \mathbf{D}\dot{\mathbf{x}}_{imp} + \mathbf{K}\Delta\mathbf{x}_{imp} = \mathbf{h}_{ext} \tag{2}$$

where $\mathbf{M}$, $\mathbf{D}$, $\mathbf{K}$ are the impedance matrices composed by both the traslational and rotational parts, $\Delta\mathbf{x}_{imp} = \mathbf{x}_{imp} - \mathbf{x}^d = [\Delta\mathbf{p}; \boldsymbol{\varphi}_{cd}]$ (where $\mathbf{x}_{imp}^d$ is the six DoFs reference for the impedance controller), and $\mathbf{h}_{ext} = [\mathbf{f}_t; \mathbf{S}_\omega^T(\boldsymbol{\varphi}_{cd})\boldsymbol{\tau}_\varphi]$.

On the basis of the initial conditions on the impedance control position ($\mathbf{x}_{imp}(t=0) = \mathbf{x}_{imp}^0$) and velocity $\dot{\mathbf{x}}_{imp}(t=0) = \dot{\mathbf{x}}_{imp}^0$), it is possible to compute the impedance control acceleration $\ddot{\mathbf{x}}_{imp}$ from (2). Such acceleration can be integrated in order to compute the Cartesian position and velocity to be used as a reference to the inner position controller.

It has to be noted that, in the proposed paper, no force/torque sensor is used in order to measure the interaction wrench vector $\mathbf{h}_{ext}$. Instead, an observer (described in Section IV) has been implemented in order to estimate the interaction joint torques $\widehat{\boldsymbol{\tau}}_{ext}$. The interaction wrench vector can then be computed as follows:

$$\widehat{\mathbf{h}}_{ext} = \mathbf{J}(\mathbf{q})^{-T}\widehat{\boldsymbol{\tau}}_{ext}, \tag{3}$$

where $\mathbf{J}(\mathbf{q})$ is the Jacobian matrix and $\mathbf{q}$ is the joint position vector. The estimated interaction wrench $\widehat{\mathbf{h}}_{ext}$ can therefore be substituted into 2 to achieved the designed compliant robot controlled behavior.

B. Inner position control

The reference Cartesian position $\mathbf{x}_{imp}$ and velocity $\dot{\mathbf{x}}_{imp}$ computed by the impedance control in the previous Section are employed to compute the joint reference signals to be provided to a PID position controller. The joint reference velocity vector $\dot{\mathbf{q}}^d$ is computed as follows [21]:

$$\dot{\mathbf{q}}^d = \mathbf{J}(\mathbf{q})^{-1}\left(\dot{\mathbf{x}}_{imp} + \mathbf{K}_{p,c}\mathbf{e}_{p,c}\right), \tag{4}$$

where $\mathbf{e}_{p,c} = \mathbf{x}_{imp} - \mathbf{x}$ is the Cartesian error, $\mathbf{x}$ is the robot end effector pose, and $\mathbf{K}_{p,c}$ is a proportional gain matrix. The PID position controller, providing the control torque $\boldsymbol{\tau}_{\text{PID}}$, can be written as:

$$\boldsymbol{\tau}_{\text{PID}} = \mathbf{K}_p\mathbf{e}_q + \mathbf{K}_d\dot{\mathbf{e}}_q + \mathbf{K}_i\int\mathbf{e}_q, \tag{5}$$

where $\mathbf{K}_p$ is the proportional gain matrix, $\mathbf{K}_i$ is the integral gain matrix, $\mathbf{K}_d$ is the derivative gain matrix, and $\mathbf{e}_q = \mathbf{q}^d - \mathbf{q}$ is the joint position error. $\mathbf{q}^d$ is obtained integrating $\dot{\mathbf{q}}^d$. The gain matrices $\mathbf{K}_p$, $\mathbf{K}_i$, $\mathbf{K}_d$ are tuned on the basis of the methodology in [22].

Exploiting the Cartesian position $\mathbf{x}_{imp}$ and velocity $\dot{\mathbf{x}}_{imp}$ computed by the impedance controller it is, therefore, possible to impose to the position-controlled robot a compliant behavior.

C. Robot dynamics compensation

The following manipulator dynamics can be considered [23]:

$$\mathbf{B}(\mathbf{q})\ddot{\mathbf{q}} + \mathbf{C}(\mathbf{q},\dot{\mathbf{q}}) + \mathbf{g}(\mathbf{q}) + \boldsymbol{\tau}_f(\dot{\mathbf{q}}) = \boldsymbol{\tau} - \mathbf{J}(\mathbf{q})^T\mathbf{h}_{ext}, \tag{6}$$

where $\mathbf{B}(\mathbf{q})$ is the robot inertia matrix, $\mathbf{C}(\mathbf{q},\dot{\mathbf{q}})$ is the robot Coriolis vector, $\mathbf{g}(\mathbf{q})$ is the robot gravitational vector, $\boldsymbol{\tau}_f(\dot{\mathbf{q}})$ is the robot joint friction vector, and $\boldsymbol{\tau}$ is the robot joint torque vector.

Based on (6), it is possible to design a position controller with robot dynamics compensation:

$$\boldsymbol{\tau} = \boldsymbol{\tau}_{\text{PID}} + \mathbf{C}(\mathbf{q},\dot{\mathbf{q}}) + \mathbf{g}(\mathbf{q}) + \boldsymbol{\tau}_f(\dot{\mathbf{q}}). \tag{7}$$

Therefore, the resulting controlled robot dynamics results in:

$$\mathbf{B}(\mathbf{q})\ddot{\mathbf{q}} = \boldsymbol{\tau}_{\text{PID}} - \mathbf{J}(\mathbf{q})^T\mathbf{h}_{ext}. \tag{8}$$

IV. EKF

To derive the proposed EKF, an augmented filter state is defined, which comprehends the robot joint velocities $\dot{\mathbf{q}}$, the robot joint positions $\mathbf{q}$, the integral of the robot joint positions $\int \mathbf{q}$, and the external joint torques τ_{ext}:

$$\mathbf{q}_a = [\dot{\mathbf{q}}^T, \mathbf{q}^T, [\int \mathbf{q}]^T, \tau_{ext}^T]^T. \tag{9}$$

The augmented filter state $\mathbf{x}_a$ is then substituted in the robot dynamics equation (8) to write the state-space interaction dynamics:

$$\dot{\mathbf{q}}_a = \begin{bmatrix} \mathbf{B}(\mathbf{q})^{-1}\mathbf{K}_d & \mathbf{B}(\mathbf{q})^{-1}\mathbf{K}_p & \mathbf{B}(\mathbf{q})^{-1}\mathbf{K}_i \\ \mathbf{0}_{7x7} & \mathbf{0}_{7x7} & \mathbf{0}_{7x7} \\ \mathbf{0}_{7x7} & \mathbf{0}_{7x7} & \mathbf{0}_{7x7} \end{bmatrix} \mathbf{q}_a^d - \begin{bmatrix} \mathbf{B}(\mathbf{q})^{-1}\mathbf{K}_d & \mathbf{B}(\mathbf{q})^{-1}\mathbf{K}_p & \mathbf{B}(\mathbf{q})^{-1}\mathbf{K}_i & \mathbf{B}(\mathbf{q})^{-1} \\ \mathbf{I}_{7x7} & \mathbf{0}_{7x7} & \mathbf{0}_{7x7} & \mathbf{0}_{7x7} \\ \mathbf{0}_{7x7} & \mathbf{0}_{7x7} & \mathbf{0}_{7x7} & \mathbf{0}_{7x7} \\ \mathbf{0}_{7x7} & \mathbf{0}_{7x7} & \mathbf{0}_{7x7} & \mathbf{0}_{7x7} \end{bmatrix} \mathbf{q}_a, \tag{10}$$

where $\mathbf{q}_a^d = [[\dot{\mathbf{q}}^d]^T, [\mathbf{q}^d]^T, [\int \mathbf{q}^d]^T]^T$.
To account for the uncertainties in the model, a variable $\boldsymbol{\nu}_a = [\boldsymbol{\nu}_{\mathbf{q}}, \boldsymbol{\nu}_{\dot{\mathbf{q}}}, \boldsymbol{\nu}_{\int \mathbf{q}} \boldsymbol{\nu}_{\tau_{ext}}]$ is included in the filter dynamics. The resulting equations represent the filter dynamics:

$$\mathbf{f}(\mathbf{q}_a, \boldsymbol{\nu}_a) = \dot{\mathbf{q}}_a = \begin{bmatrix} \mathbf{B}(\mathbf{q})^{-1}\mathbf{K}_d & \mathbf{B}(\mathbf{q})^{-1}\mathbf{K}_p & \mathbf{B}(\mathbf{q})^{-1}\mathbf{K}_i \\ \mathbf{0}_{7x7} & \mathbf{0}_{7x7} & \mathbf{0}_{7x7} \\ \mathbf{0}_{7x7} & \mathbf{0}_{7x7} & \mathbf{0}_{7x7} \end{bmatrix} \mathbf{q}_a^d - \begin{bmatrix} \mathbf{B}(\mathbf{q})^{-1}\mathbf{K}_d & \mathbf{B}(\mathbf{q})^{-1}\mathbf{K}_p & \mathbf{B}(\mathbf{q})^{-1}\mathbf{K}_i & \mathbf{B}(\mathbf{q})^{-1} \\ \mathbf{I}_{7x7} & \mathbf{0}_{7x7} & \mathbf{0}_{7x7} & \mathbf{0}_{7x7} \\ \mathbf{0}_{7x7} & \mathbf{0}_{7x7} & \mathbf{0}_{7x7} & \mathbf{0}_{7x7} \\ \mathbf{0}_{7x7} & \mathbf{0}_{7x7} & \mathbf{0}_{7x7} & \mathbf{0}_{7x7} \end{bmatrix} \mathbf{q}_a + \boldsymbol{\nu}_a, \tag{11}$$

Therefore, calling $\widehat{\mathbf{q}}_a$ the augmented state estimate, $\mathbf{C}_a$ the observation matrix for the robot joint velocity $\dot{\mathbf{q}}$ and the robot joint position $\mathbf{q}$, and $\mathbf{K}_{EKF}$ the gain matrix, the EKF is defined as:

$$\begin{cases} \dot{\widehat{\mathbf{q}}}_a = \mathbf{f}(\mathbf{q}_a, \boldsymbol{\nu}_a) + \mathbf{K}_{EKF}(\mathbf{y} - \mathbf{C}_a \widehat{\mathbf{q}}_a), \\ \widehat{\mathbf{y}} = \mathbf{h}(\mathbf{q_a}, \mathbf{w}), \end{cases} \tag{12}$$

where the gain matrix $\mathbf{K}_{EKF}$ is computed as follows:

$$\mathbf{K}_{EKF} = \mathbf{P}\mathbf{C}_a\mathbf{R}^{-1}. \tag{13}$$

$\mathbf{R}$ represents the measurements noise covariance matrix:

$$\mathbf{R} = \mathbf{H}E\{\mathbf{w}\mathbf{w}^T\}\mathbf{H}^T = \mathbf{H}\mathbf{W}\mathbf{H}^T. \tag{14}$$

The observation function $\mathbf{h}$ linearly maps the sample inaccuracies, due to measurement noise $\mathbf{w}$, through the matrix $\mathbf{H}$:

$$\mathbf{H} = \left.\frac{\partial \mathbf{h}}{\partial \mathbf{w}}\right|_{\widehat{\mathbf{q}}_a}. \tag{15}$$

The covariance matrix $\mathbf{P}$ and its rate:

$$\dot{\mathbf{P}} = \mathbf{A}_a\mathbf{P} - \mathbf{P}\mathbf{C}_a^T\mathbf{R}^{-1}\mathbf{C}_a\mathbf{P} + \mathbf{Q} + \mathbf{P}\mathbf{A}_a^T, \tag{16}$$

are based on the dynamics of the state and on the model uncertainties. Matrices $\mathbf{A}_a$ and $\mathbf{G}_a$ are defined, respectively, as:

$$\mathbf{A}_a = \left.\frac{\partial \mathbf{f}}{\partial \mathbf{q}_a}\right|_{\widehat{\mathbf{q}}_a}; \qquad \mathbf{G}_a = \left.\frac{\partial \mathbf{f}}{\partial \boldsymbol{\nu}_a}\right|_{\widehat{\mathbf{q}}_a}. \tag{17}$$

Matrix $\mathbf{Q}$, used for the estimation of the parameters, is defined as:

$$\mathbf{Q} = \mathbf{G}_a E\{\boldsymbol{\nu}_a\boldsymbol{\nu}_a^T\}\mathbf{G}_a^T = \mathbf{G}_a\mathbf{V}\mathbf{G}_a^T. \tag{18}$$

It has to be mentioned that it is possible to neglect the evaluation of the derivative $\frac{\partial \mathbf{B}(\mathbf{q})}{\partial \mathbf{q}}$ in (17). This assumption is justified for low-dynamics systems such as compliant-controlled robots (as in the case of this paper). In fact, the modification of $\mathbf{B}(\mathbf{q})$ is negligible since the robot motion has a reduced dynamics.

The proposed EKF has been discretized for its implementation and online usage [24].

Remark. It has to be highlighted that an observer for the estimation of the external interaction is proposed due to the common tasks in which compliance control is employed. In fact, Cartesian robot control is generally required for interaction applications, requiring to estimate forces and torques acting at the robot end-effector. Therefore, this observer can be also adopted for interaction control purposes [25]–[27].

V. RESULTS

The proposed interaction torques estimation methodology for position-controlled robots have been tested on a Franka EMIKA panda robot. The robot has been controlled employing the architecture described in Section III. For the implementation of the described controller, the Franka EMIKA panda robot torque-controller (with a control frequency of $1k$ Hz) has been exploited.

The outer impedance control matrices have been imposed as follows: mass parameters into the diagonal matrix $\mathbf{M}$ have been imposed equal to 5 kg, while inertia parameters have been imposed equal to 10 kg m^2; translational parameters into the diagonal stiffness matrix $\mathbf{K}$ have been imposed equal to 2000 N/m, while rotational parameters have been imposed equal to 100 Nm/rad; damping ratio parameters into the diagonal matrix $\mathbf{h}$ have been imposed equal to 1 (allowing for the definition of the damping matrix $\mathbf{D} = 2\mathbf{h}\sqrt{\mathbf{MK}}$).

The inner position control gains (optimized exploiting the approach in [22]) have been imposed as follows: $\mathbf{K}_p = diag([1000, 1500, 1500, 1500, 400, 200, 150])$ Nm/rad, $\mathbf{K}_d = diag([32, 40, 30, 45, 20, 20, 10])$ Nms/rad, $\mathbf{K}_i = diag([15, 15, 20, 40, 40, 30, 40])$ Nm/rad/s.

In order to apply external forces/torques to the robot, a human operator interacted with the robot (in compliance control). Exploiting the internal joint torque sensors of the Franka EMIKA panda robot, it has been possible to measure the external joint torques $\boldsymbol{\tau}_{ext}$ applied by the human operator,

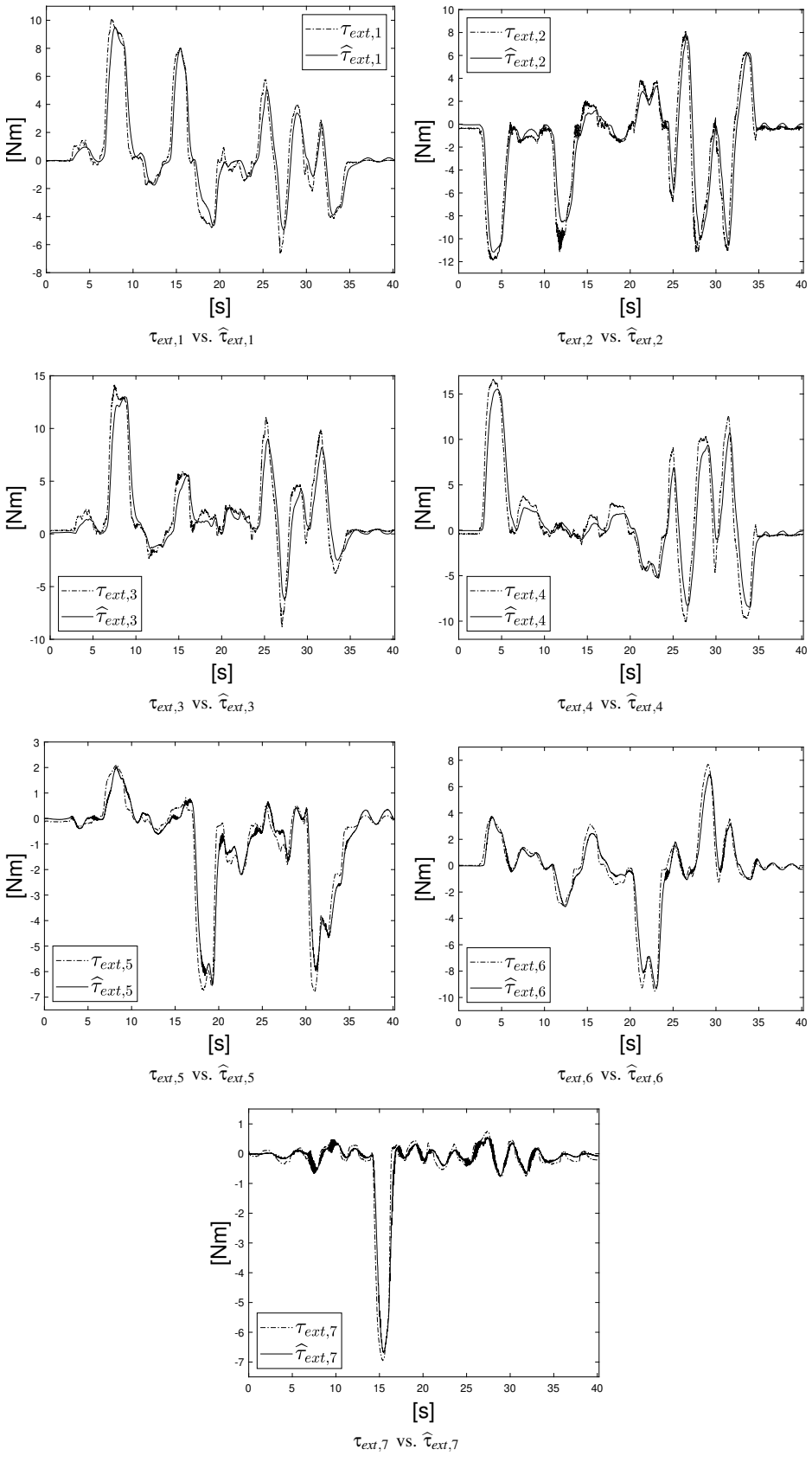

Fig. 2: Measured external joint torques $\boldsymbol{\tau}_{ext}$ (dashed line) vs. estimated external joint torques $\widehat{\boldsymbol{\tau}}_{ext}$ (continuous line).

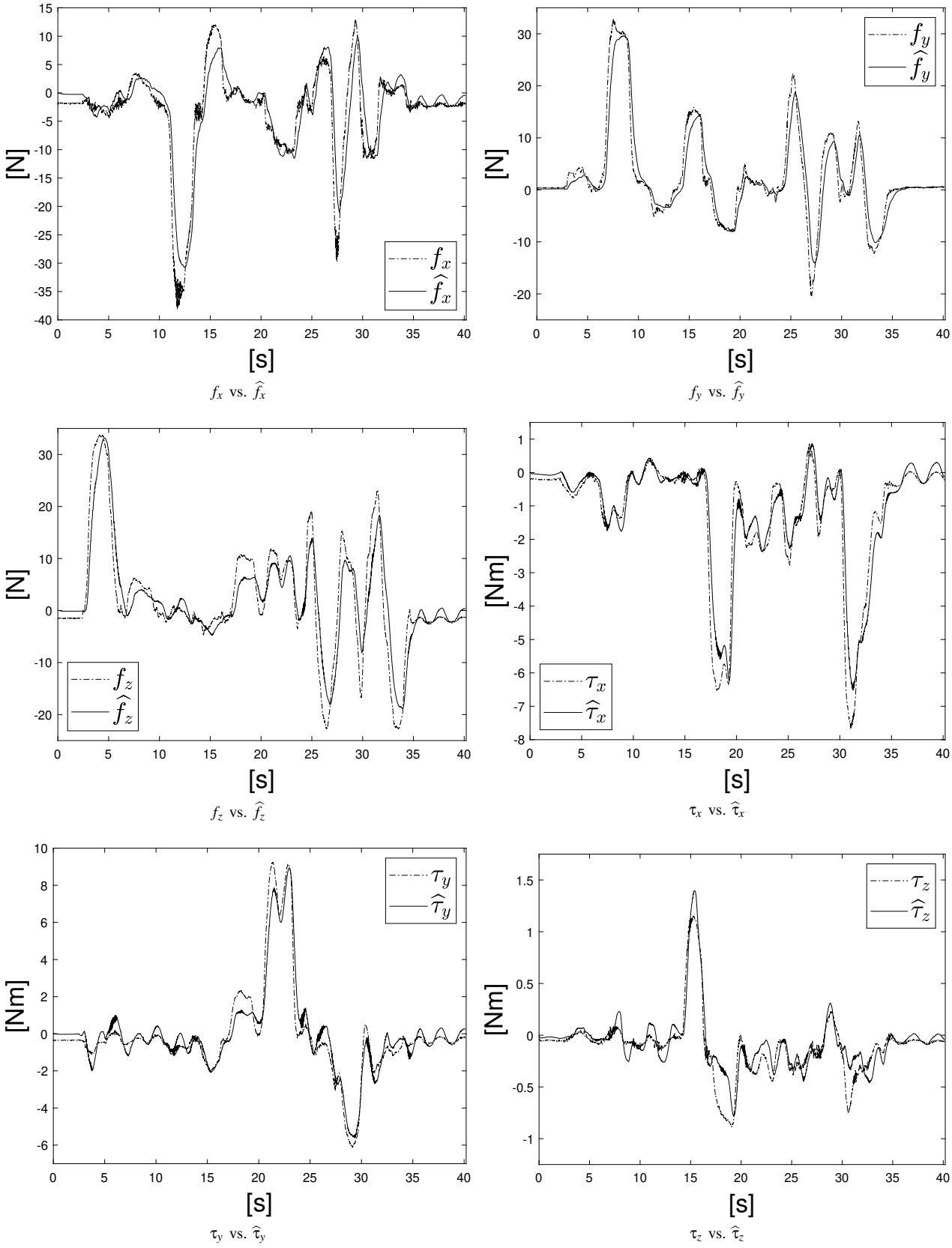

Fig. 3: Measured external wrench $\mathbf{h}_{ext}$ (dashed line) vs. estimated external joint torques $\widehat{\mathbf{h}}_{ext}$ (continuous line).

to be compared with the estimated external joint torques $\widehat{\boldsymbol{\tau}}_{ext}$ provided by the proposed EKF (Section IV). The measured external wrench vector $\mathbf{h}_{ext}$ has been computed as

$$\mathbf{h}_{ext} = \mathbf{J}(\mathbf{q})^{-T}\boldsymbol{\tau}_{ext}$$

to be compared with the estimated external wrench vector $\widehat{\mathbf{h}}_{ext}$.

Figure 2 shows the measured external joint torques $\boldsymbol{\tau}_{ext}$ vs. the estimated external joint torques $\widehat{\boldsymbol{\tau}}_{ext}$. As it can be seen from the provided plots, the proposed observer is capable to estimate the external joint torques with high accuracy and reduced delay. Such high performance are reflected into the estimation of the external wrench as shown in Figure 3. As shown in the provided plots, the external wrench is properly estimated, making it possible to use such estimation for the implementation of the proposed outer impedance controller as described in Section III-A.

VI. Conclusions

In this work, an external joint torques observer is proposed in order to implement an outer compliance controller for a sensorless position-controlled industrial robot. To this aim, an Extended Kalman Filter (EKF) is derived on the basis of the resulting controlled robot dynamics. The outer compliance controller exploits the available estimation of the external interaction. Experimental validation is provided employing a Franka EMIKA panda robot. The estimated external joint torques have been compared with the measurements from the internal joint torque sensors of the robot. An accurate estimation of the interaction is achieved, making possible to implement the proposed framework on real sensorless position-controlled manipulators for compliance control purposes.

Current/future work is devoted to exploit the proposed framework for the design of an advanced sensorless interaction controller. More in detail, an impact controller is under development. In addition, an optimal switching impact/force (OSIF) controller is under investigation.

References

[1] Z. M. Mohamed, *Flexible Manufacturing Systems: Planning Issues and Solutions*. Routledge, 2018.

[2] N. Hogan, "Impedance control: An approach to manipulation," in *1984 American control conference*. IEEE, 1984, pp. 304–313.

[3] L. Roveda, S. Haghshenas, A. Prini, T. Dinon, N. Pedrocchi, F. Braghin, and L. M. Tosatti, "Fuzzy impedance control for enhancing capabilities of humans in onerous tasks execution," in *2018 15th international conference on ubiquitous robots (UR)*. IEEE, 2018, pp. 406–411.

[4] L. Roveda, "A user-intention based adaptive manual guidance with force-tracking capabilities applied to walk-through programming for industrial robots," in *2018 15th International Conference on Ubiquitous Robots (UR)*. IEEE, 2018, pp. 369–376.

[5] ——, "Adaptive interaction controller for compliant robot base applications," *IEEE Access*, vol. 7, pp. 6553–6561, 2018.

[6] A. Janot, P.-O. Vandanjon, and M. Gautier, "A generic instrumental variable approach for industrial robot identification," *IEEE Transactions on Control Systems Technology*, vol. 22, no. 1, pp. 132–145, 2013.

[7] W.-H. Chen, D. J. Ballance, P. J. Gawthrop, and J. O'Reilly, "A nonlinear disturbance observer for robotic manipulators," *IEEE Transactions on industrial Electronics*, vol. 47, no. 4, pp. 932–938, 2000.

[8] A. Colomé, D. Pardo, G. Alenya, and C. Torras, "External force estimation during compliant robot manipulation," in *2013 IEEE International Conference on Robotics and Automation*. IEEE, 2013, pp. 3535–3540.

[9] J. Hu and R. Xiong, "Contact force estimation for robot manipulator using semiparametric model and disturbance kalman filter," *IEEE Transactions on Industrial Electronics*, vol. 65, no. 4, pp. 3365–3375, 2017.

[10] G. Peng, C. Yang, W. He, and C. L. P. Chen, "Force sensorless admittance control with neural learning for robots with actuator saturation," *IEEE Transactions on Industrial Electronics*, vol. 67, no. 4, pp. 3138–3148, 2020.

[11] M. Van Damme, P. Beyl, B. Vanderborght, V. Grosu, R. Van Ham, I. Vanderniepen, A. Matthys, and D. Lefeber, "Estimating robot end-effector force from noisy actuator torque measurements," in *2011 IEEE International Conference on Robotics and Automation*. IEEE, 2011, pp. 1108–1113.

[12] M. Linderoth, A. Stolt, A. Robertsson, and R. Johansson, "Robotic force estimation using motor torques and modeling of low velocity friction disturbances," in *2013 IEEE/RSJ International Conference on Intelligent Robots and Systems*. IEEE, 2013, pp. 3550–3556.

[13] E. Villagrossi, L. Simoni, M. Beschi, N. Pedrocchi, A. Marini, L. M. Tosatti, and A. Visioli, "A virtual force sensor for interaction tasks with conventional industrial robots," *Mechatronics*, vol. 50, pp. 78–86, 2018.

[14] M. Sharifi, H. Talebi, and M. Shafiee, "Adaptive estimation of robot environmental force interacting with soft tissues," in *2015 3rd RSI International Conference on Robotics and Mechatronics (ICROM)*. IEEE, 2015, pp. 371–376.

[15] A. Dong, Z. Du, and Z. Yan, "A sensorless interaction forces estimator for bilateral teleoperation system based on online sparse gaussian process regression," *Mechanism and Machine Theory*, vol. 143, p. 103620, 2020.

[16] E. Magrini, F. Flacco, and A. De Luca, "Estimation of contact forces using a virtual force sensor," in *2014 IEEE/RSJ International Conference on Intelligent Robots and Systems*. IEEE, 2014, pp. 2126–2133.

[17] A. Mendizabal, R. Sznitman, and S. Cotin, "Force classification during robotic interventions through simulation-trained neural networks," *International journal of computer assisted radiology and surgery*, vol. 14, no. 9, pp. 1601–1610, 2019.

[18] A. Marban, V. Srinivasan, W. Samek, J. Fernández, and A. Casals, "A recurrent convolutional neural network approach for sensorless force estimation in robotic surgery," *Biomedical Signal Processing and Control*, vol. 50, pp. 134–150, 2019.

[19] F. Caccavale, C. Natale, B. Siciliano, and L. Villani, "Six-dof impedance control based on angle/axis representations," *Robotics and Automation, IEEE Transactions on*, vol. 15, no. 2, pp. 289–300, 1999.

[20] L. Sciavicco and B. Siciliano, *Modelling and control of robot manipulators*. Springer Science & Business Media, 2012.

[21] B. Siciliano, L. Sciavicco, L. Villani, and G. Oriolo, *Robotics: modelling, planning and control*. Springer Science & Business Media, 2010.

[22] L. Roveda, M. Forgione, and D. Piga, "Robot control parameters auto-tuning in trajectory tracking applications," *Control Engineering Practice*, vol. 101, p. 104488, 2020.

[23] B. Siciliano and L. Villani, *Robot Force Control*, 1st ed. Norwell, MA, USA: Kluwer Academic Publishers, 2000.

[24] L. Roveda, N. Iannacci, and L. M. Tosatti, "Discrete-time formulation for optimal impact control in interaction tasks," *Journal of Intelligent & Robotic Systems*, vol. 90, no. 3-4, pp. 407–417, 2018.

[25] L. Roveda and D. Piga, "Robust state dependent riccati equation variable impedance control for robotic force-tracking tasks," *International Journal of Intelligent Robotics and Applications*, vol. 4, no. 4, pp. 507–519, 2020.

[26] L. Roveda, M. Magni, M. Cantoni, D. Piga, and G. Bucca, "Human–robot collaboration in sensorless assembly task learning enhanced by uncertainties adaptation via bayesian optimization," *Robotics and Autonomous Systems*, vol. 136, p. 103711, 2021.

[27] L. Roveda and D. Piga, "Sensorless environment stiffness and interaction force estimation for impedance control tuning in robotized interaction tasks," *Autonomous Robots*, pp. 1–18, 2021.